

## RESEARCH ARTICLE

# Graphene oxide/(Carboxymethylcellulose-Sodium alginate-Acrylic acid) Surface: Synthesis and Characterization for Adsorptive Removal of Azure A from Aqueous Solutions

Layth S. Jasim\*, Alaa S. Alwan

*Department of Chemistry, College of Education, University of Al-Qadisiyah, Al-Qadisiyah, Iraq*

*Received: 29th December, 2021; Revised: 08th February, 2022; Accepted: 18th February, 2022; Available Online: 25th March, 2022*

---

### ABSTRACT

Graphene oxide/(Carboxymethylcellulose-Sodium alginate-Acrylic acid) was studied as the adsorbent of Azure A dye. The time to reach the equilibrium state for Azure A adsorption on the surface of hydrogel composite GO/(CMC-SA-AAC) is 120 minutes. The rate of dye adsorption on the surface of the hydrogel composite was excellent because hydrogel composite has a large surface area to absorb the largest possible amount of dye. A pseudo-first-order and a pseudo-second-order model observed Azure A dye's adsorption kinetics on the hydrogel composite GO/(CMC-SA-AAC) surface. Illustration using the adsorption process data reflects a pseudo-second-order model. Linear forms of adsorption isotherms, Langmuir equations, Freundlich, and Timken equations were also studied. Thermodynamic effects, pH, and ionic strength effects were examined to determine the maximum absorption. Thermodynamic functions of, Enthalpy (H), Gibbs free energy (G), and Entropy (S) also were studied.

**Keywords:** Acrylic acid, Adsorption, Azure A, Carboxymethylcellulose, Hydrogel composites, Sodium alginate.

International Journal of Drug Delivery Technology (2022); DOI: 10.25258/ijddt.12.1.14

**How to cite this article:** Jasim LS, Alwan AS. Graphene oxide/(Carboxymethylcellulose-Sodium alginate-Acrylic acid) Surface: Synthesis and Characterization for Adsorptive Removal of Azure A from Aqueous Solutions. International Journal of Drug Delivery Technology. 2022;12(1):74-80.

**Source of support:** Nil.

**Conflict of interest:** None

---

### INTRODUCTION

It is widely accepted that manufactured dyes that end up in the water supply are one of the most significant water pollutants because they are used extensively in the dyeing processes of textiles, plastics, paper, food, and cosmetic products.<sup>1-4</sup> Industrial wastewater contains high concentrations of dyes, so removing these pollutants from sewage water is very necessary because it has organic and inorganic materials, toxic and carcinogenic substances, and genetic mutations, for this reason, it is not suitable for human consumption, agriculture, and others.<sup>5,6</sup> These pigments are characterized by their stability, great coloring ability, and ease of use, not to mention that they are cheaper and more versatile.<sup>7</sup> It is necessary to eliminate these pollutants, there are several physical and chemical methods to treat them, the most important of which are chemical oxidation, filtration and distillation, reverse osmosis, ion exchange, chemical and electrical precipitation.<sup>8,9</sup> High-efficiency, low-cost water treatment is the most critical application for this technique.<sup>10,11</sup>

### METHOD

#### Materials

Graphene Oxide (GO), carboxymethyl cellulose (CMC), sodium alginate (SA), acrylic acid (AAc), ferric chloride (III) ( $\text{FeCl}_3$ ), iron sulfate ( $\text{FeSO}_4$ ), potassium persulfate (KPS), Azure A from Aldrich, Potassium chloride (KCl), Sodium chloride (NaCl), Calcium carbonate ( $\text{CaCO}_3$ ). All the used reagents were pure, and deionized water was used to prepare all solutions.

#### Formulation of GO/(CMC-SA-AAc) Hydrogel Composite

Hydrogel composite GO/(CMC-SA-AAc) was prepared by preparing a set of solutions and then mixing them by dissolving (0.1 g) of carboxymethylcellulose (CMC) in (5 mL) of deionized water for 60 minutes while stirring with a magnetic stirrer. Then prepare a sodium alginate (SA) solution by dissolving (0.5 g) in (17 mL) of deionized water and stirring continuously for (60) minutes and prepare a Graphene Oxide (GO) solution by (0.005 g) dissolves in (5 mL) of deionized water and putting it in an ultrasound machine for a period of time (60) minutes.

---

\*Author for Correspondence: layth.alhayder@gmail.com

Then we prepare (KPS) by taking an amount of (0.03 g) of it and dissolving it in (2 mL) of deionized water. Finally, we prepared the crosslinking agent ( $\text{FeSO}_4$ ) by taking (1.5 g) and using a small amount of deionized water to dissolve it. Afterward, the solutions are then mixed by combining a (SA) solution to (CMC) solution with constantly stirring for 30 minutes, after that, add the (GO) solution to the created solution and stir continuously for 30 minutes. and After 30 minutes of continuous stirring, add the (AAc) solution, followed by the (KPS) solution for a period of 15 minutes. After that, we prepare (500ml) of ( $\text{FeCl}_3$ ) (10% w/v), After this, using a syringe, we distill the resulting solution into drops, then we leave the product for 360 minutes, then we wash the generated hydrogel composites with deionized distilled water until the pH=7 is achieved, then dried at a temperature of  $60^\circ\text{C}$  for 12 hours, and then ground to obtain a fixed weight of hydrogel composites.

### Studies of Adsorption

Adsorption of dye on a hydrogel composite of GO/CMC-SA-AAC with surface-adsorbed hydrogel Adsorption amount, time, pH of solution, temperature (10, 15, 20, 25), isotherms for dye adsorption on the hydrogel composite (GO/CMC-SA-AAC) adsorbent surface were all studied in detail using various dye concentrations. The results showed that all these variables had a significant impact on the rate of dye adsorption. To be able to obtain the most amount of adsorbed dye, (0.05 g) of the surface was mixed with (10 mL) of the dye solution and inserted into the shaking device. UV-visible radiation is then used to determine the dye concentrations. The amount of adsorbent on the surface of the adsorbent was calculated using the following eq. (1):

$$Q_e = \frac{V_{\text{sol}}(C_0 - C_e)}{m} \quad (1)$$

Where:

- ( $Q_e$ ): the quantity of adsorbent material (mg/g). ( $V_{\text{sol}}$ ): the total volume of the adsorbed substance's solution (L).
- ( $C_e$ ): Concentration of adsorbent material at equilibrium (mg/L).
- ( $C_0$ ): the adsorbate substance's primary consideration (mg/L), (m): The adsorbed material's weight (g).<sup>12-14</sup>

### Fourier Transform Infrared Spectroscopy (FT-IR)

The chemical structure of the (CMC-SA-AAC/GO) composite was characterized using FTIR spectroscopy. The KBr was used to detect the spectra of solid-state materials over a range of ( $400-4000$ )  $\text{cm}^{-1}$ .

## DISCUSSION OF THE RESULTS

### Characterization of GO/(CMC-SA-AAC) Hydrogel Composite

In Figures 1 and 2 FTIR spectrum of GO/(CMC-SA-AAC) hydrogel composite, the stretching vibration of ( $-\text{OH}$ ) in SA and CMC was ascribed to the wide absorption band ( $3660-3220$ )  $\text{cm}^{-1}$ . While in GO, it was attributed to the large absorption band between ( $3040$  and  $3650$ )  $\text{cm}^{-1}$ . The

asymmetric and symmetric vibrations of ( $-\text{COO}-$ ) were attributed to the bands at ( $1650$  and  $1430$ )  $\text{cm}^{-1}$ , respectively. The characteristic vibration of ( $-\text{C}-\text{O}-\text{C}-$ ) was given to the band at ( $1040$ )  $\text{cm}^{-1}$ . The stretching vibration of ( $-\text{C}-\text{H}$ ) was given to the band at ( $2920$ )  $\text{cm}^{-1}$ . And absorbance at ( $3030$ )  $\text{cm}^{-1}$  is due to the vibration stretching of the (C-H) backbone in the graphite structure, the peaks at ( $1610$  and  $1570$ )  $\text{cm}^{-1}$  are due to the stretching vibration of the (C-H). The stretching vibration of the unoxidized (C=C) groups in the carbon structure caused the peak to occur at  $1640$   $\text{cm}^{-1}$ . The stretching vibration of the ( $-\text{C}=\text{O}$ ) bond in the carboxylic groups was attributed to the peak at  $1720$   $\text{cm}^{-1}$ . The stretching vibration of ( $-\text{C}=\text{C}$ ) caused the peak at  $1680$   $\text{cm}^{-1}$ . The typical absorption bands of ( $-\text{C}-\text{O}-\text{C}$ ) were found at ( $1010$  and  $840$ )  $\text{cm}^{-1}$ . The bending vibration of ( $-\text{O}-\text{H}$ ) was attributed for the peak at ( $740$ )  $\text{cm}^{-1}$ .<sup>15-18</sup>

### Contact Time Effect

The adsorption time of the Azure A dye is illustrated on the surface of the hydrogel composite adsorbent GO/(CMC-SA-

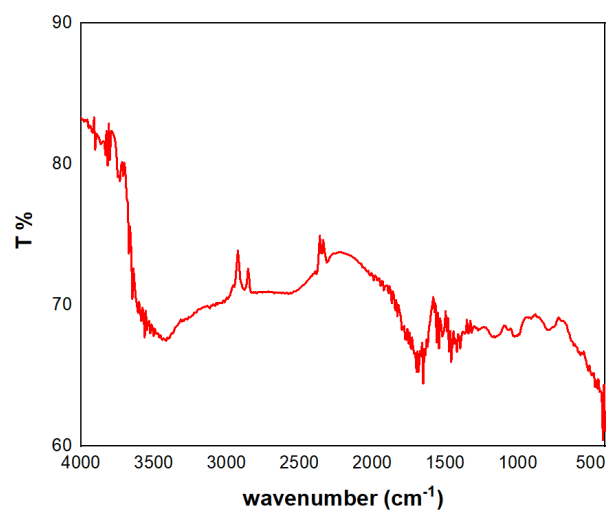


Figure 1: FTIR spectra of GO/(CMC-SA-AAC) before adsorption of Azure A

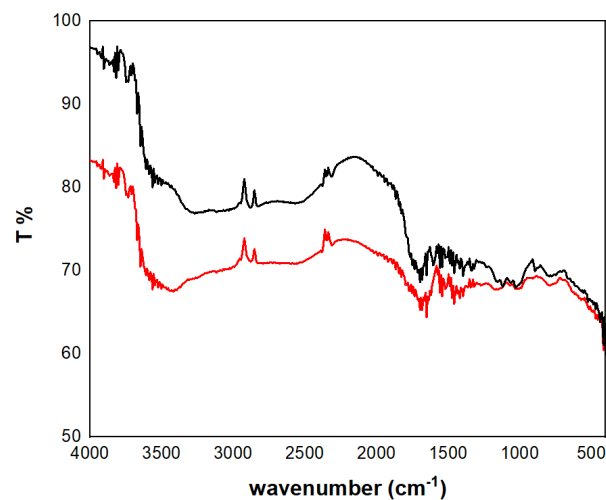


Figure 2: FTIR spectra of GO/(CMC-SA-AAC) after adsorption of Azure A

AAc). As the time spent in contact with the solution on the adsorbent surface increases, the adsorbent surface becomes more adsorbent, as shown in Figure 3, the amount of adsorbent material increased.

**Adsorption of the Azure A Dye**

To illustrate the dye adsorption process on the surface at 25°C, the dye concentration was plotted against the amount of adsorbent. This is due to the presence of active groups on the surface that can absorb the dye.<sup>19,20</sup> As shown in Figure 4, the amount of dye that was absorbed on the surface was excellent.<sup>21</sup>

**Adsorption Isotherm of Azure A**

As illustrated in Figure 5, According to the Giles classification, the adsorption process refers to the (S) class. The adsorbent

material on the surface of the adsorbent material are vertical or inclined in this type, and the surface is heterogeneous. The Freundlich, Langmuir, and Timken equations were used to interpret a result of the adsorption process at 25°C, as illustrated in Figures 5, 6, and 7, respectively. The results revealed that the adsorption of Azure A dye on the adsorbent’s surface is similar to the Freundlich isotherm. The correlation coefficients and isotherms for Langmuir, Freundlich, and Timken are shown in Table 1.<sup>22-24</sup>

**Thermodynamic Effects**

Increasing the temperature increases the amount of adsorbents on the surface of the adsorbent, and this leads to the adsorption

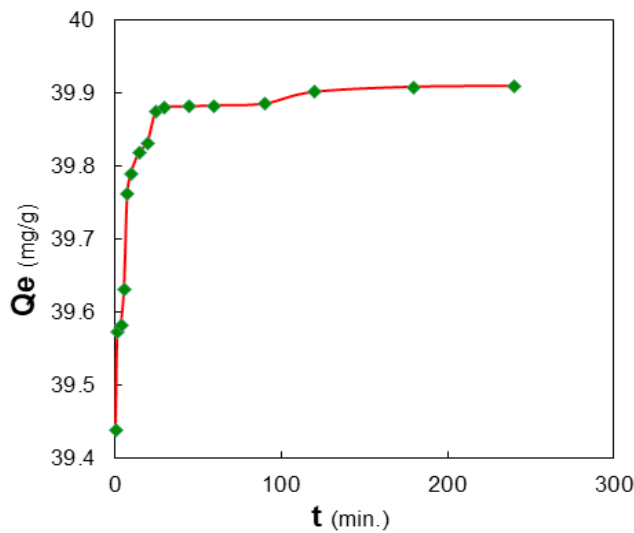


**Figure 3:** The effect of changing the adsorption time of azure A dye on the adsorbent surface at 120 min, 25°C, (0.05g) of dye in (10 mL) water (200 ppm) and pH=7

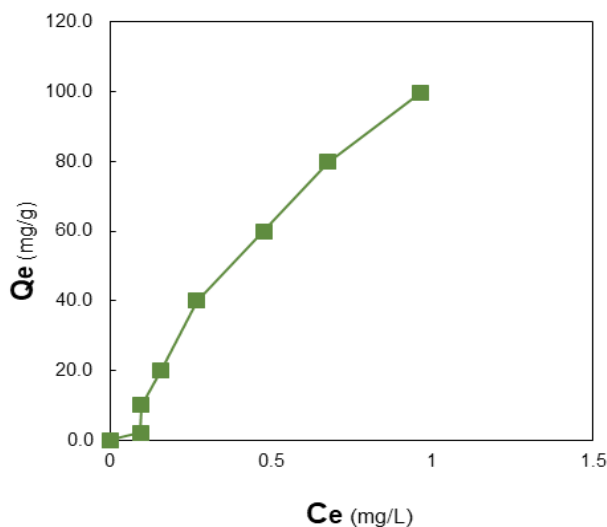


**Figure 4:** The adsorption isotherm for Azure A dye at (25°C), (pH=7), and (120 minutes)

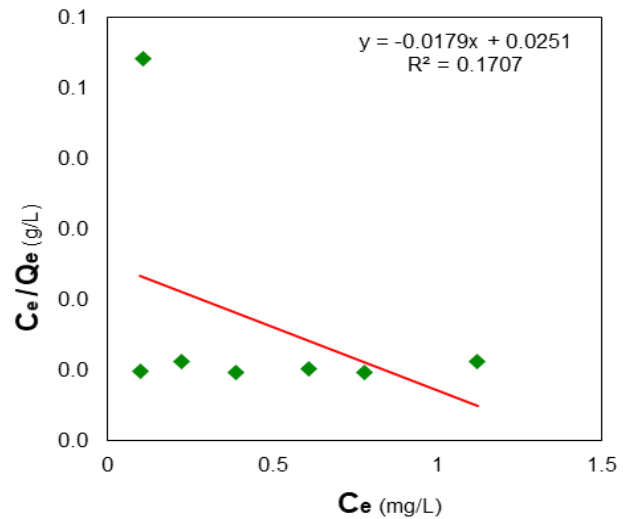


**Figure 5:** Langmuir isotherm for Azure A dye adsorption on the surface hydrogel composite GO/(CMC-SA-AAc)

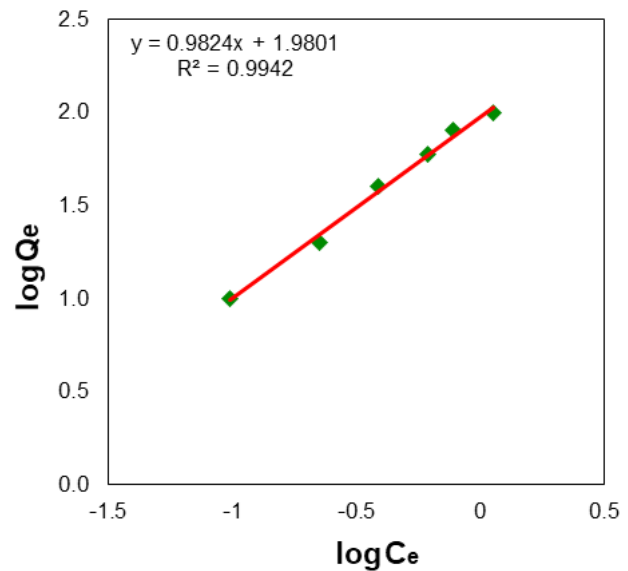


**Figure 6:** Freundlies isotherm for Azure A dye adsorption on the surface hydrogel composite GO/(CMC-SA-AAc)

**Table 1:** The coefficients and constants of correlation Timken, Freundlies, and Langmuir isotherms of Azure A dye adsorption on surface hydrogel composite GO/(CMC-SA-AAC)

Equation of Langmuir			Equation of Freundlich			Equation of Timken		
$K_L$	$q_m$	$R^2$	$K_F$	$N$	$R^2$	$K_T$	$B$	$R^2$
-0.7131	-55.865	0.860	95.521	1.0179	0.946	9.8135	37.253	0.835

**Table 2:** The amount of Azure A dye absorbed at surface hydrogel composite GO/(CMC-SA-AAC) at various temperatures

10°C		15°C		20°C		25°C	
$C_e$ (mg/L)	$Q_e$ (mg/g)	$C_e$ (mg/L)	$Q_e$ (mg/g)	$C_e$ (mg/L)	$Q_e$ (mg/g)	$C_e$ (mg/L)	$Q_e$ (mg/g)
0	0	0	0	0	0	0	0
0.214	1.957	0.224	1.955	0.107	1.978	0.094	1.981
0.347	9.930	0.289	9.942	0.098	9.980	0.096	9.980
0.613	19.877	0.552	19.889	0.224	19.955	0.159	19.968
0.751	39.849	0.555	39.888	0.387	39.922	0.269	39.946
1.341	59.731	1.101	59.779	0.611	59.877	0.478	59.904
2.403	79.519	1.872	79.625	0.780	79.844	0.677	79.864
3.480	99.303	2.379	99.524	1.122	99.775	0.964	99.807

**Table 3:** The temperature affect the highest adsorption of Azure A dye on surface hydrogel composite GO/(CMC-SA-AAC)

$T^{\circ}C$	$T_k$	$1000/T(K^{-1})$	$C_e=63$	
			$X_m$	$\ln(X_m)$
5	278	3.533569	10	2.302585
15	288	3.472222	20	2.995732
20	293	3.412969	35.5	3.569533
25	298	3.355705	40	3.688879

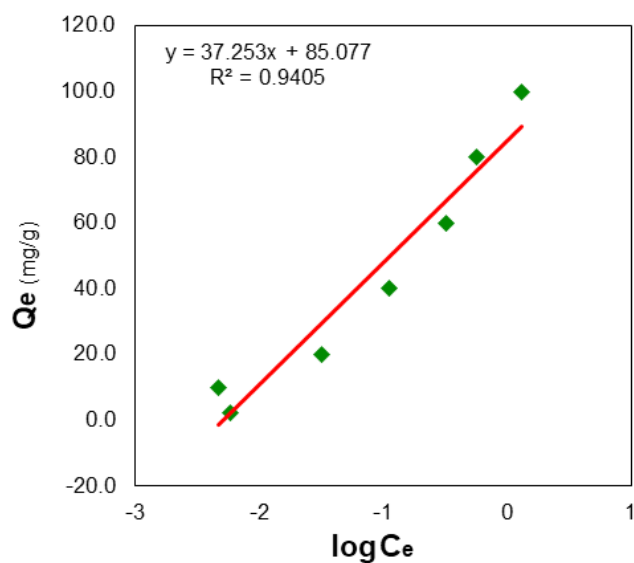


**Figure 7:** Timken isotherm for Azure A dye adsorption on the surface hydrogel composite GO/(CMC-SA-AAC)

process being endothermic, as shown in Table 2 and Figure 8. As the temperature increases, the degree of viscosity in the solution decreases, allowing the adsorbate to spread more widely across the surface. The molecules' kinetic energy increases as the temperature increases, increasing the chances of interacting with the active sites and allowing more molecules to pass through the adsorbent material's pores (Table 3).<sup>25-28</sup>

The functions of thermodynamics, as well as the change in free energy(G), enthalpy(H), and entropy(S), were determined in Table 4. The results revealed that the enthalpy(H) value had increased positively, indicating an endothermic reaction. The adsorption process is spontaneous because the free energy is negative. A random increase of the molecule's adsorbate caused

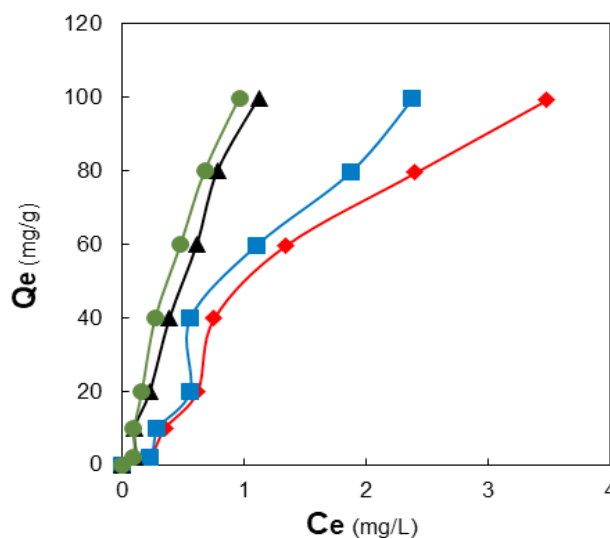


**Figure 8:** Amount of Azure A dye adsorbed at surface hydrogel composite GO/(CMC-SA-AAC) at various temperatures

by an increase in kinetic energy is shown by a positive charge increase in entropy.<sup>29</sup>

**The Effect of Ionic Strength**

Because of the interaction between a salt ion utilized and solvent molecules, a decrease in the solubility of the dye in

the solution leads to an increase in the amount of adsorbate on the surface with an increase in the salt concentration in the solution, as shown in Table 5 and Figures 9 and 10. The salt ions in the double layer increase adsorption of adsorbate molecules on the surface. When it comes to interacting with the solvent, salt ions and dye ions compete.<sup>30,31</sup>

**Adsorption Kinetic**

Two kinetic equations, pseudo-first-order and pseudo-second-order, were used to study the Azure A dye’s adsorption kinetics on the absorbent’s surface. According to correlation coefficients ( $R^2$ ), As illustrated in Table 6 and Figures (11 a and b), the pseudo-second-order kinetic equation is more compatible with the dye adsorption kinetics on the surface.<sup>32,33</sup>

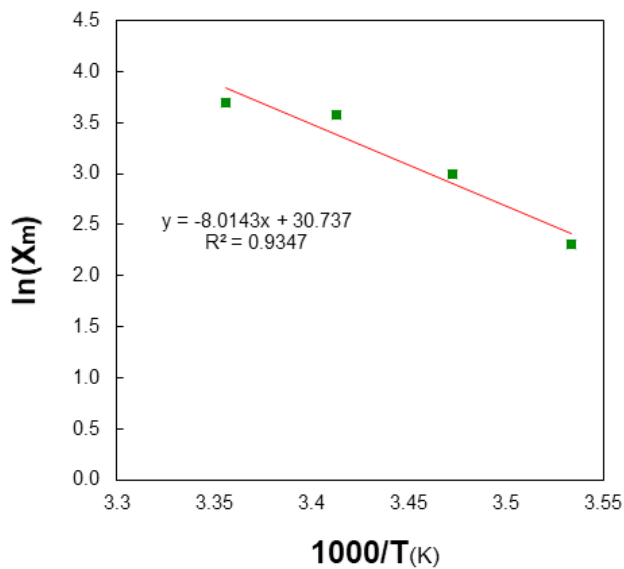


**Figure 9:** Plot  $\ln X_m$  vs. the adsorption AzureA dye’s absolute temperature on the surface hydrogel composite GO/ (CMC-SA-AAC)

**Table 4:** Parameters of thermodynamics of the Azure A dye adsorption process on the surface hydrogel composite GO/(CMC-SA-AAC)

$H$ ( $kJ.mol^{-1}$ )	$G$ ( $kJ.mol^{-1}$ )	$S$ ( $J.mol^{-1}.K^{-1}$ )	Equilibrium constant ( $K$ )
+6.662	-13.011	271.818	83.529

**Table 5:** The effect of ionic strength on Azure A dye adsorption on the surface hydrogel composite GO/(CMC-SA-AAC)

$C_e$ ( $mg/g$ )	$NaCl$ ( $mol/L$ )	$Q_e$ ( $mg/g$ )	$KCl$ ( $mol/L$ )	$Q_e$ ( $mg/g$ )	$CaCO3$ ( $mol/L$ )	$Q_e$ ( $mg/g$ )
200	0	39.908	0	39.908	0	39.908
200	0.005	39.841	0.005	39.853	0.005	39.902
200	0.01	39.748	0.01	39.839	0.01	39.897
200	0.03	39.744	0.03	39.773	0.03	39.821
200	0.05	39.626	0.05	39.738	0.05	39.723
200	0.10	39.475	0.10	39.650	0.10	39.718
200	0.15	39.424	0.15	39.603	0.15	39.675
200	0.20	39.396	0.20	39.577	0.20	39.616

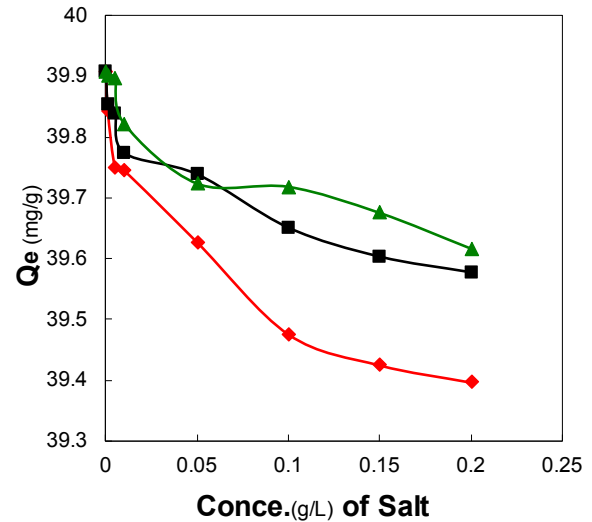
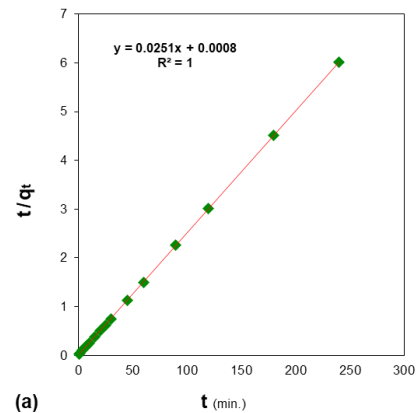
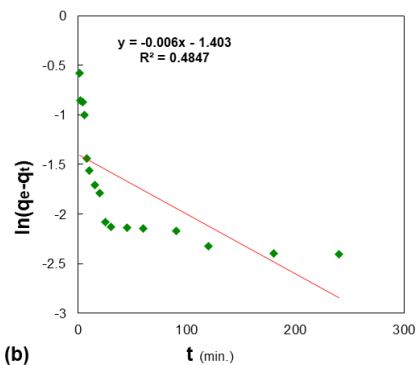


**Figure 10:** Salt’s effect on Azure A dye adsorption on the surface hydrogel composite GO/(CMC-SA-AAC)



(a)



(b)

**Figure 11:** (a) Pseudo first order model (b) Pseudo second order model of Azure A dye adsorption on the GO/(CMC-SA-AAC)

**Table 6:** Illustrate the pseudo first order and pseudo second order correlation coefficients and kinetic constants of Azure A dye adsorption on the surface hydrogel composite GO/(CMC-SA-AAC)

Pseudo first order			Pseudo second order			$H$
$K_1$	$q_e$	$R^2$	$K_2$	$q_e$	$R^2$	
0.006	0.245	0.484	0.787	39.840	1	1250

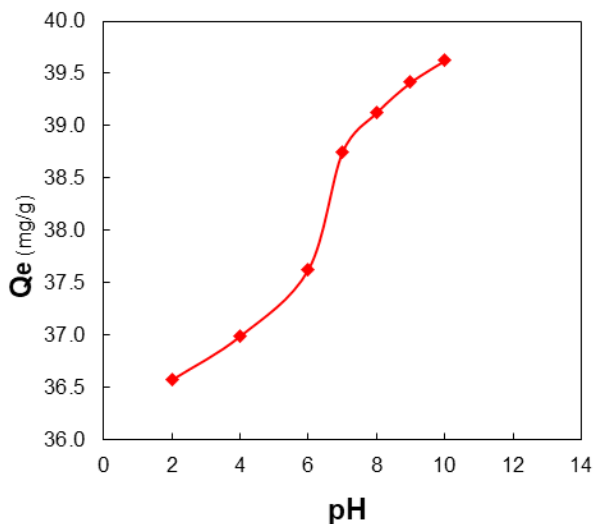


Figure 12: The pH effect on Azure A adsorption

### The pH Effect

Figure 12 illustrates the data of a study into the effect of the acidic function of a solution on the amount of adsorbate on the adsorbent's surface. A pretreatment solution with a (1–10) pH range was used (10 mL samples). We mixed for 120 minutes at room temperature with a dye concentration of (200 mg/L) and a composite GO/(CMC-SA-AAC) of (0.05 g). We then use a UV-vis Spectrum to measure the adsorption after centrifuging the liquids and extracting the sample with a microsyringe.<sup>34,35</sup>

### CONCLUSIONS

The use of a GO/(CMC-SA-AAC) hydrogel composite as an adsorbent for the Azure A dye was studied. Fourier transform infrared spectroscopy was used to characterize the composite hydrogels that were synthesized (FTIR). The adsorption capacity of composite hydrogels was influenced by contact time, ionic strength, temperature, and solution pH. The process of dye adsorption on the surface of the adsorbent is identical to Freundlich's isotherm. According to the results, the adsorption process follows a pseudo-second order model. To determine out what the maximum adsorption is. The thermodynamic functions of the adsorption process, Entropy (S), Enthalpy (H) and Gibbs free energy (G), were also studied.

### REFERENCES

1. Ma, X., Cui, W., Yang, L., Yang, Y., Chen, H. and Wang, K. 2015 *Bioresource technology* 185 70 -78.
2. Dil, E.A., Ghaedi, M., Ghezelbash, G.R., Asfaram, A. and Purkait, M.K. 2017 *Journal of industrial and engineering chemistry* 48 162-172.
3. Tamez, C., Hernandez, R. and Parsons, J.G. 2016 *Microchemical Journal* 125 97-104.
4. Azimi, A., Azari, A., Rezakazemi, M. and Ansarpour, M. 2017 *ChemBioEng Reviews* 4 (1) 37-59.
5. Dil, E.A., Ghaedi, M., Ghezelbash, G.R., Asfaram, A., Ghaedi, A.M. and Mehrabi, F. 2016 *RSC Advances*. 6 (59) 54149-54161.
6. Dil, E.A., Ghaedi, M., Asfaram, A. and Mehrabi, F. 2017 *Ultrasonics Sonochemistry* 36 409-419.
7. Luan, J., Hou, P.X., Liu, C., Shi, C., Li, G.X. and Cheng, H.M. 2016 *Journal of Materials Chemistry A* 4(4) 1191-1194.
8. Chandran, D. 2016 *Int. J. Sci. Eng. Res* 7 392-403.
9. Karimifard, S. and Moghaddam, M.R.A. 2016 *Process Safety and Environmental Protection* 99 20-29.
10. Khan, T.A., Nazir, M., Ali, I. and Kumar, A. 2017 *Arabian Journal of Chemistry* 10 S2388-S2398.
11. A I Atyaa, ND Radhy, L S Jasim. "Synthesis and Characterization of Graphene Oxide/Hydrogel Composites and Their Applications to Adsorptive Removal Congo Red from Aqueous Solution", *Journal of Physics: Conference Series*, 2019.
12. Kumar, Bijender, and Yuvraj Singh Negi. "Water absorption and viscosity behaviour of thermally stable novel graft copolymer of carboxymethyl cellulose and poly (sodium l-hydroxy acrylate)." *Carbohydrate polymers* 181 (2018): 862-870.
13. Liu, M., Li, X., Du, Y. and Han, R. 2018 *Bioresource Technology Reports*.
14. Kumar, Bijender, et al. "Nanoporous Sodium Carboxymethyl Cellulose-g-poly (Sodium Acrylate)/FeCl<sub>3</sub> Hydrogel Beads: Synthesis and Characterization." *Gels* 6.4 (2020): 49.
15. Luo X, Lei X, Cai N, Xie X, Xue Y, Yu F. Removal of heavy metal ions from water by magnetic cellulose-based beads with embedded chemically modified magnetite nanoparticles and activated carbon. *ACS Sustain Chem Eng*. 2016;4(7):3960-3969. 38.
16. Leshaf A, Cherif HZ, Benmansour K. Adsorption of acidol red 2BE-NW dye from aqueous solutions on carboxymethyl cellulose/organo-bentonite composite: characterization, kinetic and thermodynamic studies. *J Polym Environ*. 2019;27(5):1054-1064. 36.
17. Yadav M, Rhee KY, Park S. Synthesis and characterization of graphene oxide/carboxymethylcellulose/alginate composite blend films. *Carbohydr Polym*. 2014;110:18-25.
18. Moussa I, Khiari R, Moussa A, Belgacem MN, Mhenni MF. Preparation and characterization of carboxymethyl cellulose with a high degree of substitution from agricultural wastes. *Fibers Polym*. 2019;20(5):933-943. 37.
19. Safaa H. Ganduh, R.Q.K., Makarim A. Mahdi, Aseel M Aljeboree, Layth S. Jasim, Selective Spectrophotometric Determination of 4-amino Antipyrine Antibiotics in Pure Forms and their Pharmaceutical Formulations. *International Journal of Drug Delivery Technology*, 2021. 11(2): p. 371-375.
20. Zheng, Y., Wang, H., Cheng, B., You, W. and Yu, J. 2018 *Journal of Alloys and Compounds* 750 644-654.
21. Aliabadi, R.S. and Mahmoodi, N.O. 2018 *Journal of Cleaner Production* 179 235-245.
22. Munagapati, V.S. and Kim, D.S. 2017 *Ecotoxicology and environmental safety* 141 226-234.
23. Jaism, L.; Radhy, N.; Kmal, R. A study of Adsorption of Azure B and C from Aqueous Solutions on Poly (Acryl amide-co-Crotonic acid) Hydro gels Surface. *Chem. and Pro. Eng. Research*, 2015, 32: 62-69.
24. Shu, J., Wang, Z., Huang, Y., Huang, N., Ren, C. and Zhang, W. 2015 *Journal of Alloys and Compounds* 633 338-346.
25. Dai, H., et al., Synthesis and response of pineapple peel carboxymethyl cellulose-g-poly (acrylic acid-co-acrylamide)/graphene oxide hydrogels. *Carbohydrate polymers*, 2019. 215Akinola, L.K., Ibrahim, A. and Chadi, A.S. 2016.

26. Y.Bulut, H.Aydin, A kinetic and thermodynamic study of methylene blue on wheat shell Desalination, 194, pp.259-267, 2006.
27. Makarim A. Mahdi, A.M.A., Layth S. Jasim, Ayad F. Alkaim, Synthesis, Characterization and Adsorption Studies of a Graphene Oxide/Polyacrylic Acid Nanocomposite Hydrogel. *NeuroQuantology* 2021. 19(9): p. 46-54.
28. V. Gopal, K.P. Elango, Kinetic and thermodynamic investigations of adsorption of fluoride onto activated Aloe vera carbon, *Journal of Indian Chem., Soc.*, 84(11), p.114-118, 2007.
29. Lei, C., Zhu, X., Zhu, B., Jiang, C., Le, Y. and Yu, J. 2017 *Journal of hazardous materials* 321 801-811.
30. Hu, Z., Chen, H., Ji, F. and Yuan, S. 2010 *Journal of Hazardous Materials* 173 (1-3) 292-297.
31. Lorenc-Grabowska, E. and Gryglewicz, G. 2007 *Dyes and pigments* 74 (1) 34-40.
32. Liu X, Sun J, Xu X, Alsaedi A, Hayat T, Li J. Adsorption and desorption of U (VI) on different-size graphene oxide. *Chem Eng J.* 2019;360:941-950. 46.
33. Salih SS, Ghosh TK. Adsorption of Zn(II) ions by chitosan coated diatomaceous earth. *Int J Biol Macromol.* 2018;106: 602-610.
34. Aseel M Aljeboree, R.A.M., Makarim A. Mahdi, Layth S. Jasim, Ayad F. Alkaim, Synthesis, Characterization of P(CH/AA-co-AM) and Adsorptive Removal of Pb (II) ions from Aqueous Solution: Thermodynamic Study. *NeuroQuantology* 2021. 19(7): p. 137-143.
35. Li, J., Ng, D.H., Song, P., Kong, C., Song, Y. and Yang, P. 2015 *Biomass and Bioenergy* 75 189-200.